Project 1: Reflection and Refraction

Gianfranco Grillo

September 13th, 2017

Abstract

We present the results of a series of experiments designed to study the reflection and refraction properties of a flat mirror, water, a prism, and a slab, with the latter two sharing an identical composition. There are six experiments in total. The first attempts to verify the law of reflection, the second finds the refractive index of tap water at room temperature, and the remaining four find the refractive index of the prism and slab's glass using different methods. Our results agree with expectations to varying degrees, and find that in particular the different methods for finding the refractive index of the glass significantly vary in terms of their relative accuracy.

1 Introduction

Understanding the propagation of electromagnetic waves at the interface between two media is one of the most important areas of inquiry in optics. During reflection and refraction, an electromagnetic wave changes speed and direction as it comes into contact with the interface, in the first case propagating back into the original medium, while in the second propagating from the original medium into the new one. In practice, both reflection and refraction occur whenever an electromagnetic wave is incident on a surface, as part of the wave's energy is transmitted from one medium to the other, and another part of it is reflected. We will see that we can measure the refractive index of a material in several different ways by exploring how the material reflects and transmits light via relatively simple experiments.

This paper is divided as folllows. Section 2 gives an overview of the background theory and geometry required to understand each of the experiments performed, with derivations of the equations used and the physical basis behind them. Section 3 describes the experimental setup for each of the experiments, and section 4 presents the results obtained and the procedures used in the reduction of the data. Section 5 analyses the results. Finally, we develop general conclusions in Section 6.

2 Theoretical background

2.1 Law of reflection

The law of reflection is the statement that the angle of reflection θ_r of the wave, due to its scattering as it impinges on a flat surface, is equal to its angle of incidence θ_i.

$$\theta_i = \theta_r \tag{1}$$

A simple derivation of this law can be found in [1]. Both of these angles are measured with respect to the normal of the surface that performs the reflection of the wave. Note that this law applies only when the mirror is large compared to the wavelength of the wave, enabling the electrons at the surface to oscillate in phase with each other when they absorb and emit the energy carried by the wave. In the context of this project, this condition holds, so we expect the law of reflection to apply.

2.2 Snell's Law and index of refraction of water

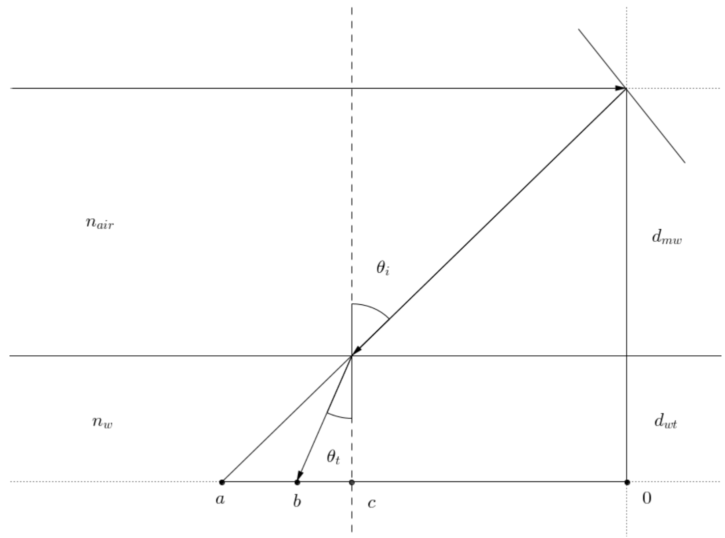

Figure 1: Geometry for experiment 2

Snell's Law relates the refractive indices of two media to the respective incident and transmitted angles of a ray of light as it propagates from one medium to the other. Let the refractive index of the originating medium be n_i and the refractive index of the medium into which the wave propagates be n_t, and let the incident and transmitted angles at the interface be θ_i and θ_t, respectively, and according to Snell's Law

$$n_i \sin\theta_i = n_r \sin\theta_t \tag{2}$$

We see that the law of reflection can be recovered from this statement, since in the case of reflection, $n_i = n_r$, and thus it follows that the incidence angle is equal to the "transmitted" angle, which in this case is the reflected angle. A proper derivation of Snell's Law can be found in [1]. Note that the refractive index n of a material is related to the speed of light in vacuum c and the speed of light in the medium v by

$$n = \frac{c}{v} \tag{3}$$

which implies that light travels at different velocities in different media. The refractive index of air $n_{air} \approx 1$, a fact that will be used extensively throughout this work. In the second experiment of this report, we will use Snell's Law and the geometry shown in Figure 1 in order to find the refractive index of water n_w. Define $d_{mt} = d_{mw} + d_{wt}$, and we have that

$$\theta_i = \arctan\left(\frac{a}{d_{mt}}\right) \tag{4}$$

$$\theta_t = \arctan\left(\frac{b-c}{d_{wt}}\right) \tag{5}$$

The rules for similar triangles allow us to write c as

$$c = \frac{ad_{mw}}{d_{mt}} \tag{6}$$

By Snell's law,

$$n_w = \frac{n_{air}\sin\theta_i}{\sin\theta_t} = \frac{\sin\theta_i}{\sin\theta_t} \tag{7}$$

Combining equations (4)-(7) gives

$$\begin{aligned} n_w &= \frac{\sin\left[\arctan\left(\frac{a}{d_{mt}}\right)\right]}{\sin\left[\arctan\left(\frac{b}{d_{wt}} - \frac{ad_{mw}}{d_{wt}d_{mt}}\right)\right]} \\ &= \frac{a}{bd_{mt} - ad_{mw}}\sqrt{\frac{(bd_{mt} - ad_{mw})^2 + d_{mt}^2 d_{wt}^2}{a^2 + d_{mt}^2}} \end{aligned} \tag{8}$$

2.3 Minimum angle of deviation

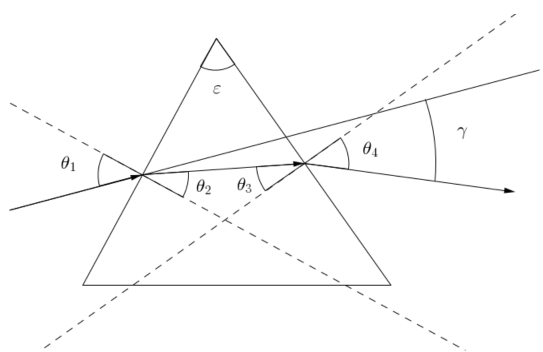

Figure 2: Geometry for experiment 3

The index of refraction n of a transparent triangular prism can be calculated by determining the angle of minimum deviation δ_{min}, which can be derived from the geometry of Figure 2. From the figure, it can be seen that ε and the angles θ_2 and θ_3 are related by

$$(90^\circ - \theta_2) + \varepsilon + (90^\circ - \theta_3) = 180^\circ \tag{9}$$

$$\varepsilon = \theta_2 + \theta_3 \tag{10}$$

Whereas the angle of deviation γ is given by

$$\delta = (\theta_1 - \theta_2) + (\theta_4 - \theta_3) = \theta_1 + \theta_4 - \varepsilon \tag{11}$$

By symmetry, δ_{min} must occur when $\theta_1 = \theta_4$, which in turn implies that $\theta_2 = \theta_3$, which means that equations (10) and (11) become

$$\varepsilon = 2\theta_2 \tag{12}$$
$$\delta_{min} = 2\theta_1 - \varepsilon \tag{13}$$

Using Snell's Law and taking into account that the medium to either side of the prism is air, we have that

$$\sin\theta_1 = n\sin\theta_2 \tag{14}$$

Solving for n, and using equations (12) and (13), we obtain a way for calculating the refractive index of the prism

$$n = \frac{\sin\left(\frac{\delta_{min}+\varepsilon}{2}\right)}{\sin\left(\frac{\varepsilon}{2}\right)} \tag{15}$$

2.4 Index of refraction of a glass slab

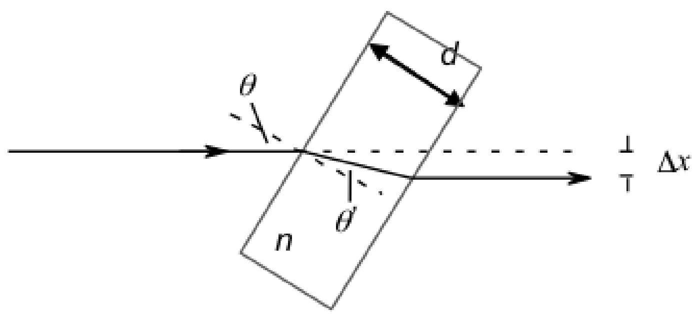

Figure 3: Geometry for experiment 4

The relationship between the index of refraction of a transparent glass slab of length d oriented at an angle θ with respect to the incident beam of light and the displacement Δx, as shown on Figure 3, can be derived again via Snell's Law. As described in [2], we have that Δx is given by

$$\Delta x = (d\tan\theta - d\tan\theta')\cos\theta = d\sin\theta\left[1 - \frac{\cos\theta}{\sqrt{n^2 - \sin^2\theta}}\right] \tag{16}$$

For the purposes of this experiment, is it useful to rewrite this equation as

$$\frac{\Delta x}{d} = \sin\theta\left[1 - \frac{\cos\theta}{\sqrt{n^2 - \sin^2\theta}}\right] \tag{17}$$

2.5 Total internal reflection

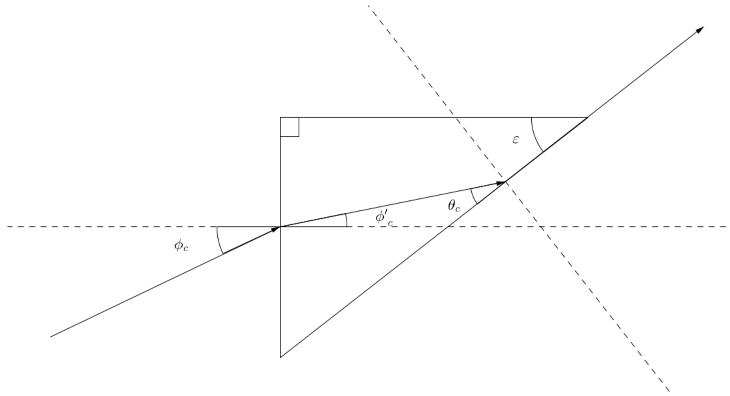

Figure 4: Geometry for experiment 5

The phenomenon of total internal reflection occurs when a ray of light propagating from a medium with refractive index n_i into a medium with refractive index n_t such that $n_i > n_t$ is completely reflected back towards the original medium, that is, the transmitted intensity of the beam is equal to zero. The minimum angle at which this happens is known as the critical angle $\theta_i = \theta_c$, for which $\theta_t = 90°$. By Snell's Law,

$$\sin\theta_i = \frac{n_t}{n_i}\sin\theta_t \to \sin\theta_c = \frac{n_t}{n_i} \tag{18}$$

In the present experiment, $n_i = n$ will be the refractive index of a 90° transparent glass prism, and $n_t = n_{air}$, so (18) becomes

$$\sin\theta_c = \frac{1}{n} \tag{19}$$

Now let a beam of light impinge on one of the faces of the prism with an angle ϕ_c as depicted in Figure 4. The geometry of the setup gives the following equation relating the angles ε, ϕ'_c, and θ_c:

$$\varepsilon - \phi'_c - \theta_c = 0 \tag{20}$$

By Snell's law, we have that

$$\sin\phi'_c = \frac{\sin\phi_c}{n} \tag{21}$$

Combining equations (19)-(21) gives

$$\frac{1}{n} = \sin(\varepsilon - \phi'_c) = \sin\left[\varepsilon - \arcsin\left(\frac{\sin\phi_c}{n}\right)\right] \tag{22}$$

Applying the trigonometric identities $\sin(a-b) = \sin(a)\cos(b) - \cos(a)\sin(b)$ allows us to write

$$\begin{aligned}\frac{1}{n} &= \sin\varepsilon\cos\left[\arcsin\left(\frac{\sin\phi_c}{n}\right)\right] - \cos\varepsilon\sin\left[\arcsin\left(\frac{\sin\phi_c}{n}\right)\right] \\ &= \sin\varepsilon\cos\left[\arcsin\left(\frac{\sin\phi_c}{n}\right)\right] - \frac{\cos\varepsilon\sin\phi_c}{n} \end{aligned} \tag{23}$$

And since $\cos\left[\arcsin\left(a\right)\right]=\sqrt{1-a^2}$,

$$\frac{1}{n}=\sin\varepsilon\sqrt{1-\frac{\sin^2\phi_c}{n^2}}-\frac{\cos\varepsilon\sin\phi_c}{n}$$

Some further elementary algebra yields the following expression for n^2

$$n^2=\sin^2\phi_c+\left(\frac{1+\cos\varepsilon\sin\phi_c}{\sin\varepsilon}\right)^2 \tag{24}$$

Expanding the square of the expression in parenthesis and adding yields

$$\begin{aligned} n^2 &= \frac{1+2\cos\varepsilon\sin\phi_c+\cos^2\varepsilon\sin^2\phi_c+\sin^2\varepsilon\sin^2\phi_c}{\sin^2\varepsilon} \\ &= \frac{1+2\cos\varepsilon\sin\phi_c+\sin^2\phi_c\left(\cos^2\varepsilon+\sin^2\varepsilon\right)}{\sin^2\varepsilon} \end{aligned}$$

Finally, using the identity $\cos^2 a+\sin^2 a=1$ gives

$$\begin{aligned} n^2 &= \frac{\cos^2\varepsilon+\sin^2\varepsilon+2\cos\varepsilon\sin\phi_c+\sin^2\phi_c}{\sin^2\varepsilon} \\ &= 1+\frac{\cos^2\varepsilon+2\cos\varepsilon\sin\phi_c+\sin^2\phi_c}{\sin^2\varepsilon} \\ n &= \sqrt{1+\left(\frac{\cos\varepsilon+\sin\phi_c}{\sin\varepsilon}\right)^2} \end{aligned} \tag{25}$$

2.6 Reflectivity

The reflectivity R of an interface is defined as the ratio of the intensities of the reflected wave and the incident wave, I_r and I_0

$$R=\frac{I_0}{I_r} \tag{26}$$

The relationship between a material's refraction index and it's reflection coefficient, assuming the material is surrounded by air, can be derived as follows. An electromagnetic wave incident on the material is, in general, reflected and refracted, with part of the wave's energy being transmitted into the material, and part of it being reflected back towards the original medium from which it came from. For a wave polarized in such a way that the electric field $\vec{E}$ is perpendicular to the plane of incidence, the tangential components of the electric field at either side of the interface are continuous, or in other words,

$$\vec{E}_{0i}+\vec{E}_{0r}=\vec{E}_{0t} \tag{27}$$

where the quantities on the left hand side are the magnitudes of the incident and reflected electric fields, respectively, and the one on the right hand side is the magnitude of the transmitted electric field. The electric field is related to the magnetic field $\vec{B}$ via

$$\hat{k}\times\vec{E}=v\vec{B} \tag{28}$$

where $\hat{k}$ is a unit vector pointing in the direction of propagation, and v is the velocity of the wave. This implies that the magnetic field of the wave points parallel to the interface. Ampere's Law provides another equation by demanding that the tangential component of $\frac{\vec{B}}{\mu}$ be continuous across the two media. The constant μ is the magnetic permeability of the material. This implies that

$$\frac{-B_i}{\mu_i}\cos\theta_i + \frac{B_r}{\mu_i}\cos\theta_r = \frac{-B_t}{\mu_t}\cos\theta_t \tag{29}$$

which, when combined with equation (27), yields

$$\frac{1}{\mu_i v_i}(E_i - E_r)\cos\theta_i = \frac{1}{\mu_t v_t}E_t\cos\theta_t \tag{30}$$

Using equation (3) and the fact that $\vec{E} = \vec{E}_0 e^{i(\vec{k}\cdot\vec{r}-\omega t)}$, we can write

$$\frac{n_i}{\mu_i}(E_{0i} - E_{0r})\cos\theta_i = \frac{n_t}{\mu_t}E_{0t}\cos\theta_t \tag{31}$$

combined with equation (30), we have

$$\left(\frac{E_{0r}}{E_{0i}}\right)_\perp = \frac{\frac{n_i}{\mu_i}\cos\theta_i - \frac{n_t}{\mu_t}\cos\theta_t}{\frac{n_i}{\mu_i}\cos\theta_i + \frac{n_t}{\mu_t}\cos\theta_t} \tag{32}$$

An analysis along the same lines allows us to calculate the same ratio for the case of the electric field being parallel to the plane of incidence, which is

$$\left(\frac{E_{0r}}{E_{0i}}\right)_\parallel = \frac{\frac{n_t}{\mu_i}\cos\theta_i - \frac{n_i}{\mu_t}\cos\theta_t}{\frac{n_t}{\mu_i}\cos\theta_i + \frac{n_i}{\mu_t}\cos\theta_t} \tag{33}$$

For the case of transition between air and glass, $\mu_i \approx \mu_t \approx \mu_0$, and the equations simplify to

$$\left(\frac{E_{0r}}{E_{0i}}\right)_\perp = \frac{n_i\cos\theta_i - n_t\cos\theta_t}{n_i\cos\theta_i + n_t\cos\theta_t} \tag{34}$$

$$\left(\frac{E_{0r}}{E_{0i}}\right)_\parallel = \frac{n_t\cos\theta_i - n_i\cos\theta_t}{n_t\cos\theta_i + n_i\cos\theta_t} \tag{35}$$

The reflectivities $R_\perp$ and $R_\parallel$ correspond to the square of these equations, because the intensity of the wave corresponds to the squared magnitude of the electric field. For the case of normal incidence, $\theta_i = \theta_t = 90°$, and using $n_i = n_{air} = 1$, we have that

$$R_\perp = R_\parallel = \left(\frac{1-n}{1+n}\right)^2 = \left(\frac{n-1}{n+1}\right)^2 \tag{36}$$

Finally, we have that for unpolarized light, $R = \frac{1}{2}\left(R_\perp + R_\parallel\right)$, and thus

$$R = \left(\frac{n-1}{n+1}\right)^2 \tag{37}$$

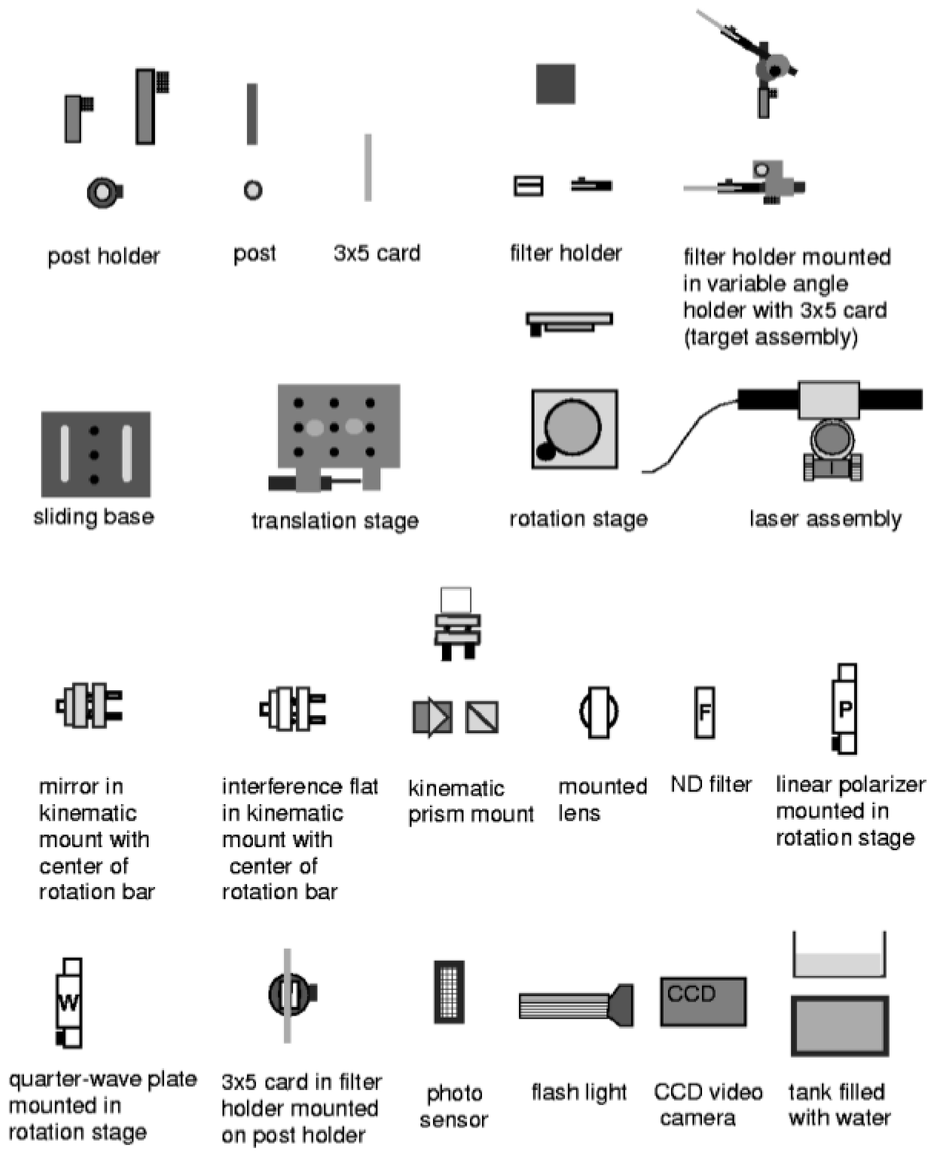

Figure 5: List of symbols

3 Experimental setup

3.1 Experiment 1

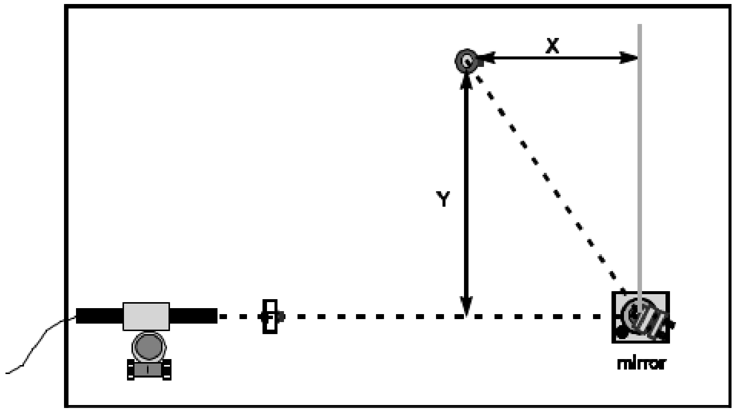

Figure 6: Setup for experiment 1

Figure 6 shows the setup used for experiment 1. The meaning of all symbols used in the setup diagrams for the experiments can be found in Figure 5. We use a 0.5 ND filter to dim the beam of light by a factor of approximately 3, and set up the flat mirror on a rotation stage as seen in the figure. The rotation stage and the mirror are initially positioned in such a way that the laser is reflected back upon itself. The nominal value of the wavelength of the monochromatic red light emitted from the laser is 632.8 nm, and the same laser is used throughout all five experiments. The setup's geometry implies that the reflected angle θ_r is given by

$$\theta_r = 90^\circ - \theta_i - \arctan\left(\frac{X}{Y}\right) \tag{38}$$

where θ_i is the incident angle as measured by the rotation stage, and X and Y are the x and y components of the distance from the mirror to the post holder as depicted in the figure. We measure the distances by counting the number of 1/4"-20 holes on the breadboard atop which the experiment takes place.

3.2 Experiment 2

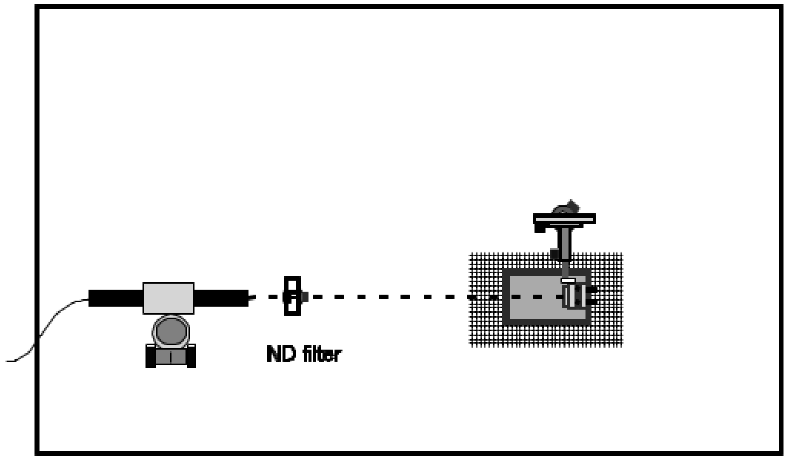

Figure 7: Setup for experiment 2

The setup for the second experiment can be seen on Figure 7. We set up the laser and the filter just as we did in experiment 1, and locate a flat mirror on top of a rotation stage that is perpendicular to the table, such that the mirror is able to reflect the laser beam from a certain height towards the table. The rotation stage and the mirror are initially set up in order for the mirror to be able to reflect the beam such that it strikes the table at an angle of $0°$ with respect to the normal to the table. This spot is taken to be the origin of the coordinate system shown in Figure 1. We mark this on a piece of graph paper fixed to the top of the table. The graph paper is evenly divided in $1\,mm^2$ squares. Next, we measure the distance d_{mt} between the place in the mirror that is hit by the laser beam and the surface of the table. We proceed to fill a circular glass container with tap water, and measure the distance d_{wt} between the surface of the water and the base of the container. The mirror is then deviated such that the beam strikes the table at an angle, and we measure the distance a between the origin and the new striking spot. Finally, we place the water tank on top of the table in between the laser beam and its surface, and record the new location b of the laser spot as seen from above. We repeat this for different values of a, produced by rotating the mirror.

3.3 Experiment 3

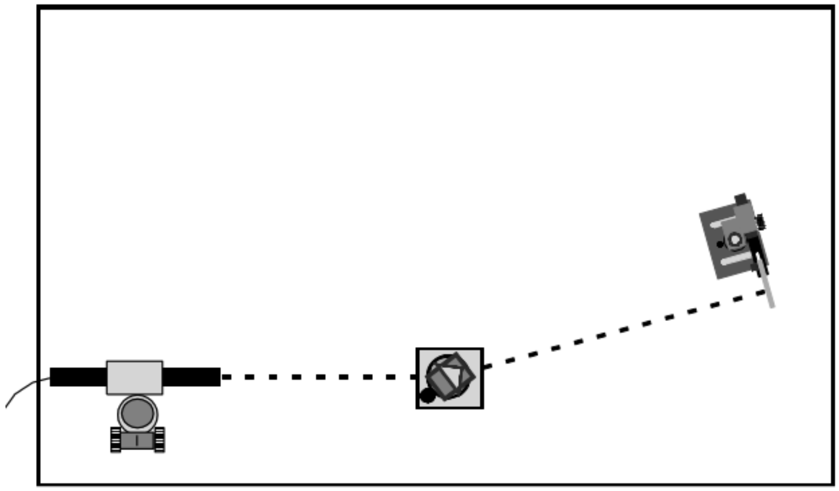

Figure 8: Setup for experiment 3

Figure 8 shows the setup for experiment 3. We place the laser in the same position as in previous experiments, and position the glass prism in a pedestal on top of a rotation stage, at the height of the laser beam. The starting position of the prism is such that the beam is normally incident with respect to its longer side. A beam stopper is placed behind the prism on top of a translation stage, as indicated in the figure. We proceed to measure the angle of minimum deviation δ_{min} by rotating the stage with the prism into a position in which any further rotation to either side results in an increase in the deviation. We calculate the angle by measuring the horizontal and vertical distances between the prism and the location of the spot at minimum deviation, X and Y. Thus, in terms of the measured variables, equation (15) is written as

$$n = \frac{\sin\left(\frac{\arctan\left(\frac{Y}{X}\right)+\varepsilon}{2}\right)}{\sin\left(\frac{\varepsilon}{2}\right)} \tag{39}$$

We use a nominal value for ε of $45°$.

3.4 Experiment 4

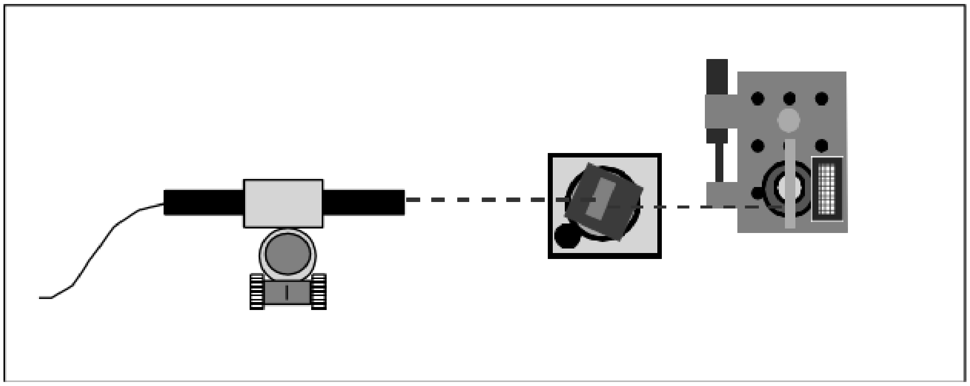

Figure 9: Setup for experiment 4

Experiment 4's setup is depicted in Figure 9. The idea behind the setup is to reproduce the geometry shown on Figure 3 for the incident angle θ and the displacement Δx in order to calculate the refraction index n of the glass prism using equation (17). We place the glass slab on a pedestal attached to a rotation stage initially set such that the incident beam is normal to one of the long faces of the slab, which is verified by ensuring that the reflected beam hits the laser aperture. A razor bladed mounted on a beam stopper is located atop the translation stage directly in front of a photosensor as shown in the figure. The razor blade is positioned in such a way that it blocks half of the beam's intensity. Then, the slab is rotated until the intensity of the light reaching the photosensor diminishes significantly with respect to the intensity recorded in the previous step, at which point the translation stage is translated until the photosensor's reading comes back to its original value. The difference in positions is recorded by the micrometer attached to the stage. This is repeated several times in order to obtain multiple data points. The distance d between the slab's faces is measured with a ruler.

3.5 Experiment 5

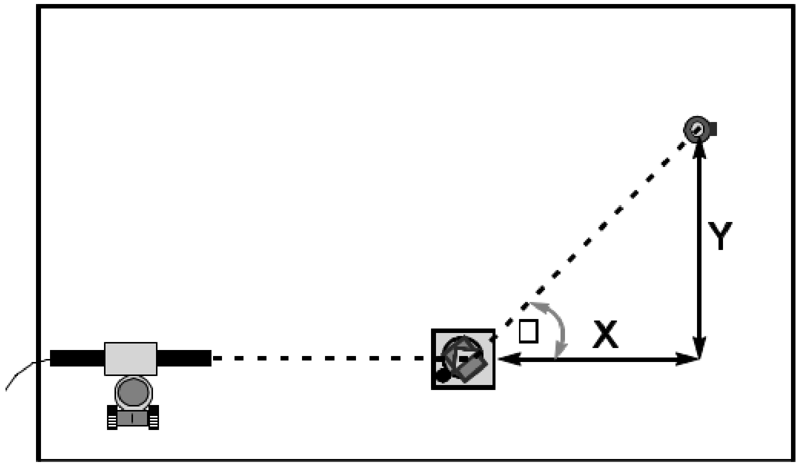

Figure 10: Setup for experiment 5

Experiment 5's setup, shown in Figure 10, is designed to replicate the geometry from Figure 4, in order to be able to find ϕ_c and apply equation (25). The setup is simple: we place the prism at the same height of the laser beam on top of a rotation stage with an initial orientation like the one shown in the figure, and rotate the stage until the transmitted beam disappears. ϕ_c is then calculated in two ways: first, by calculating the angle $\alpha = \arctan\left(\frac{Y}{X}\right)$, and then by directly reading it off the rotation stage, with the post holder in the figure being located at the position at which the transmitted beam disappears. The relationship between α and ϕ_c is given by $\phi_c = \alpha + \varepsilon - 90° = \arctan\left(\frac{Y}{X}\right) + \varepsilon - 90°$, and equation (25) becomes

$$n = \sqrt{1 + \left[\frac{\cos\varepsilon + \sin\left(\arctan\left(\frac{Y}{X}\right) + \varepsilon - 90°\right)}{\sin\varepsilon}\right]^2} \tag{40}$$

3.6 Experiment 6

3.6.1 Part A

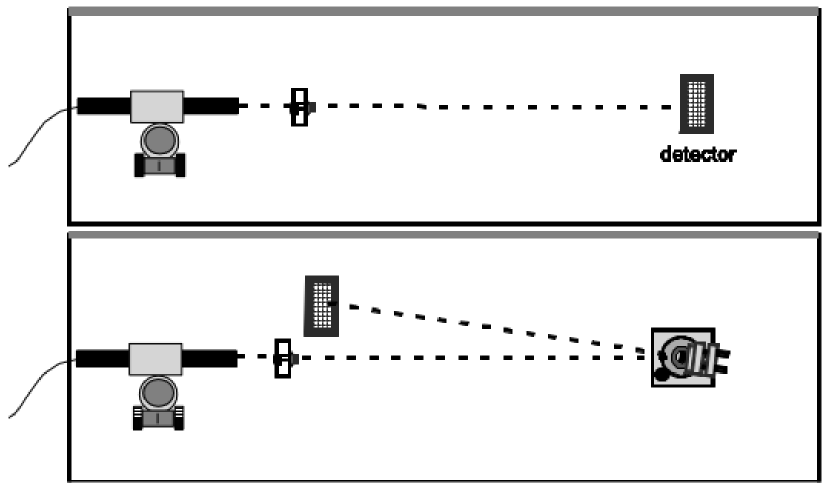

Figure 11: Setup for experiment 6A

Part A of this experiment is an attempt to measure the reflectivity of a flat mirror because it is to be used later in order to be able to calculate the reflectivity of the glass prism. Since it is not possible to measure the reflectivity at normal incidence directly without blocking the laser beam, we attempt to calculate it by first measuring the intensity I_0 of the unreflected beam, and then mounting the mirror in a rotation stage and measuring the reflected intensity I_r at small angles θ, in order to be able to extrapolate to the case of normal incidence. This is shown in Figure 11.

3.6.2 Part B

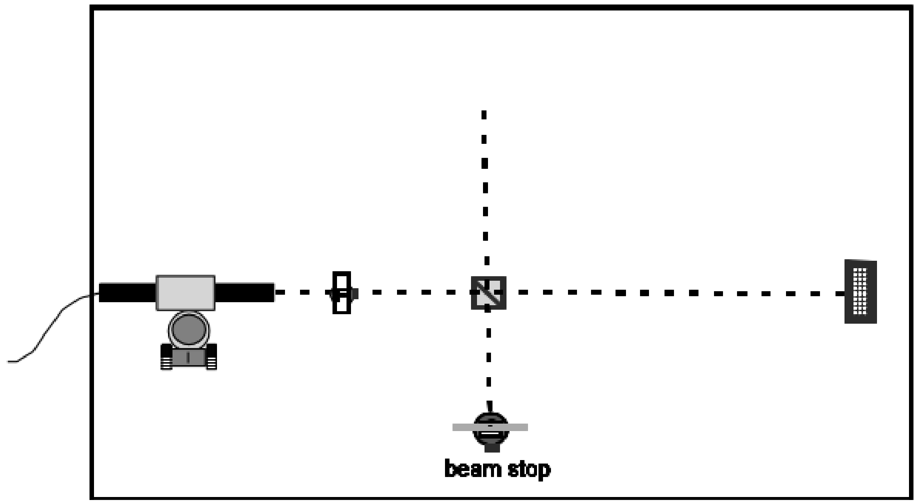

Figure 12: Setup for experiment 6B

Here, we place a beam splitter in between the laser and the mirror, as shown in Figure 12, and measure the intensity I_{bs} of the beam that emerges from the right side of the beam splitter. Thus, we are able to calculate the transmission coefficient of the beam splitter $T_{bs} = \frac{I_0}{I_{bs}}$. This part of the experiment, as will be seen, was not actually necessary.

3.6.3 Part C

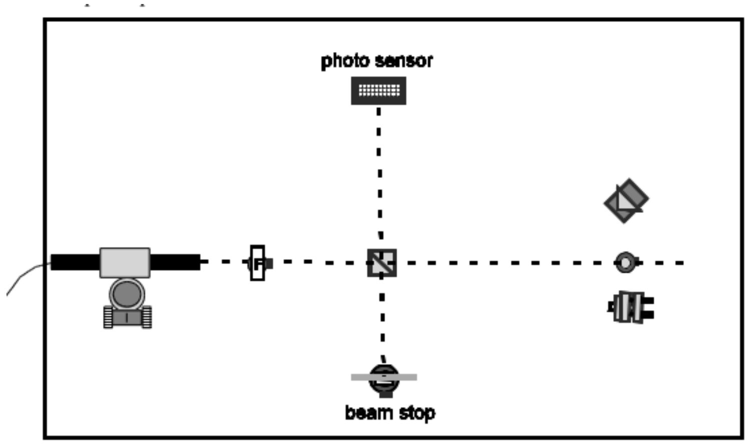

Figure 13: Setup for experiment 6C

In the third part of the experiment, we use two different setups in order to be able to calculate the reflectivity of the prism, R_p. Starting with the arrangement from Part B, we now place the photosensor 90 degrees from where it was, and place the mirror in the photosensor's original position. We then measure the intensity I_1 of the light that reaches the photosensor in this setup. Next, we perform the same procedure but with the prism instead of the mirror, and measure an intensity I_2. A naive analysis of the optical system would suggest that the equations for I_1 and I_2 would be

$$I_1 = I_0 T_{bs} R_m R_{bs} \tag{41}$$
$$I_2 = I_0 T_{bs} R_p R_{bs} \tag{42}$$

where R_m corresponds to the reflectivity of the flat mirror, and R_{bs} corresponds to the reflectivity of the mirror when the beam is incident from the right.

A more careful examination, however, leads to the conclusion that equation (42) is incorrect. Due to the geometry of the prism, when the beam strikes one of its shorter sides at normal incidence, the transmitted wave undergoes a double reflection with the two other sides that adds to the intensity of the light reflected by the first air/glass interface. Let the incident beam have an intensity I_i, and we have that the reflected intensity I_r is actually given by

$$I_r = 2R_p I_i \tag{43}$$

In this case, $I_i = I_0 T_{bs}$, which implies that the correct expression for I_2 is

$$I_2 = 2I_0 T_{bs} R_p R_{bs} \tag{44}$$

Combining equations (41) and (44) and solving for R_p gives

$$R_p = \frac{I_2 R_m}{2I_1} \tag{45}$$

which illustrates why part B of this experiment was unnecessary. Now we can apply equation (37) and solve for n in terms of R_p, which gives

$$n = \frac{-1 - R_p \pm 2\sqrt{R_p}}{R_p - 1} \tag{46}$$

The sign ambiguity is inevitable, but in practice we end up using the negative sign because otherwise we get a value of n that is less than unity.

3.6.4 Part D

The final part of the experiment involved repeating the procedure described in part A but substituting the flat mirror with the prism in order to find R_p by the same extrapolation process. Again, care must be taken to account for the geometric effect described in the previous section.

4 Results

4.1 Procedures for data reduction and error analysis

We use two different approaches to reducing the data measured. In the case of the experiments in which we can gather multiple data points, we apply the orthogonal distance regression (ODR) module of the Python library SciPy [3]. This is a good way of accounting for the fact that our measurements have errors in both the dependent and the independent variables. The idea behind this algorithm is to minimize the merit function

$$\chi^2 = \sum_{i=0}^{N-1} \left[\frac{y_i - \sum_{k=0}^{M-1} f(x_i, \vec{p})}{\sigma_{xi}^2 + \sigma_{yi}^2} \right]^2 \tag{47}$$

where y_i is the measured value of the dependent variable, x_i is the independent variable,σ_{xi} and σ_{yi} a measure of their their standard deviations (taken to be their measurement error), and $f(x_i, \vec{p})$ an arbitrary model function of the independent variables and a vector of parameters $\vec{p}$. ODR is based on the Levenberg-Marquardt method described in [4], and this particular implementation is able to provide a best fit and a standard deviation for the values of the parameters in the model, which we will identify with the values of the quantities that we are trying to calculate from the experiment, as will be seen below. A more detailed examination of ODR is beyond the scope of this work and can be found in [5].

For the cases in which we have only one (experiment 3) or two (experiment 5) data points, we calculate the value of the quantity that we are trying to find simply by writing it in terms of the dependent and independent variables and applying error propagation. In the particular case of experiment 5, we calculate the two values for the refractive index independently.

In both cases we use the Python uncertainties package [6] in order to perform error propagation. This package allows us to calculate errors for complicated expressions that depend on the measured experimental quantities, whose errors we estimate from the practical difficulty of the corresponding measurement and the precision of the instrument used in order to perform it.

4.2 Experiment 1

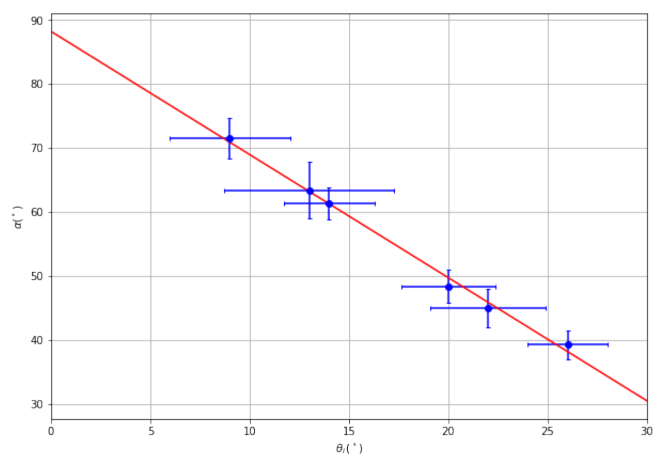

Figure 14: α vs incident angle θ_i. The data points are in blue and the line in red represents the best fit for parameter n of the model given in (48).

From equation (45), we find that plotting $\alpha = \arctan\left(\frac{x}{y}\right)$ as a function of θ_i should be a straight line with a slope $m = -2$ line and a y-intercept $b = 90°$, if the law of reflection holds, since with $\theta_i = \theta_r$, we have that

$$\arctan\left(\frac{X}{Y}\right) = -2\theta_i + 90^\circ \tag{48}$$

The deviation from such a line gives us a way of estimating how far from flat the mirror used is, and the subsequent deviation from the law. Figure 14 shows this plot. The best fit estimates for m and b returned by the ODR algorithm are $m = -1.92 \pm 0.08$ and $b = 88 \pm 2^\circ$. The errors for the measurements were estimated as 0.5 holes for the X and Y measurements, due mainly to the fact that the mirror was not directly on top of a hole, and $\pm 1^\circ$ for θ_i, a reasonable estimate given the scale of the rotation stage.

4.3 Experiment 2

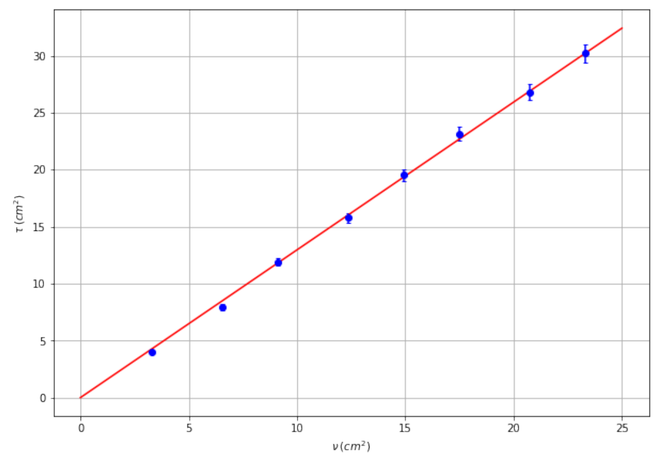

Figure 15: τ vs ν. The data points are in blue and the line in red represents the best fit for parameter n of the model given in (49).

$a\,(cm)$	1.00	2.00	3.00	4.00	5.00	6.00	7.00	8.00
$b\,(cm)$	0.95	1.90	2.80	3.75	4.65	5.55	6.50	7.40

Table 1: Measured values for a and b ($\pm 0.05\,cm$). The measured vertical distance parameters were $d_{mt} = 14.5 \pm 0.1\,cm$ and $d_{wt} = 4.0 \pm 0.1\,cm$

To perform the analysis, we rearrange equation (8) as

$$a\sqrt{\frac{(bd_{mt} - ad_{mw})^2 + d_{mt}^2 d_{wt}^2}{a^2 + d_{mt}^2}} = (bd_{mt} - ad_{mw})n_w \tag{49}$$

and define the quantities $\tau = a\sqrt{\frac{(bd_{mt}-ad_{mw})^2+d_{mt}^2 d_{wt}^2}{a^2+d_{mt}^2}}$ and $\nu = bd_{mt} - ad_{mw}$, turning (49) in a simple relationship, $\tau = n_w\nu$. Plotting τ vs ν should then give a straight line that passes throught the origin with slope n_w. The result of such a plot is given in Figure 15. Since τ and ν are combinations of the measured variables and parameters a, b, d_{mt} and d_{mw}, we also present the raw measurements for a and b in Table 1. The errors in the measurements for a and b were estimated as to be consistent with the scale of the graph paper used to measure the distances, which was subdivided in 1 mm squares; as such $\Delta a = \Delta b = \pm 0.5\, mm$. An error of $\pm 1\, mm$ was chosen for d_{mt} and d_{mw}, which were measured using a ruler with subdivisions of 1 mm, but which were in practice harder to measure accurately than a and b. The ODR algorithm gives a value for the refraction index of water $n_w = 1.298 \pm 0.008$.

4.4 Experiment 3

This experiment is simpler than the previous two because the refraction index of the prism n depends only on the constants ε and δ_{min}, which means that given ε, we can only measure δ_{min} once in order to determine n. We take $\varepsilon = 45 \pm 1°$ and our measurements for X and Y are $X = 29.5 \pm 0.1\, cm$ and $Y = 14.1 \pm 0.1\, cm$, so applying equation (47), we get a value of $n = 1.51 \pm 0.01$.

4.5 Experiment 4

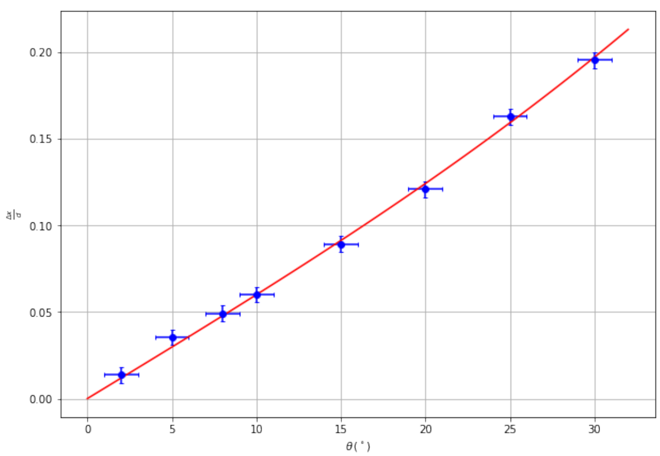

Figure 16: $\Delta x/d$ vs θ. The data points are in blue and the line in red represents the best fit for parameter n of the model given in (17).

From equation (17), we can calculate the value of n by plotting $\frac{\Delta x}{d}$ as a function of θ, and then find the n that minimizes the residuals of the merit function (47) with $f(x_i, \vec{p}) = f(\theta_i, n) = \sin\theta_i \left[1 - \frac{\cos\theta_i}{\sqrt{n^2 - \sin^2\theta_i}}\right]$. Figure 16 shows a plot of $\frac{\Delta x}{d}$ as a function of θ together with a best fit line calculated using the best fit value of n given by the ODR algorithm, $n = 1.514 \pm 0.009$. We estimated the errors in Δx to be $\pm 0.05\, mm$, mainly due to the difficulty in getting the voltage in the photosensor to be exactly equal to its value at $\theta = 0°$. The measured value for the slab's width was $d = 11 \pm 0.5$ mm, and the error for the measurement of θ was taken as $1°$, as was done in the previous experiments.

4.6 Experiment 5

We calculate n in two ways, again using only single measurements: by measuring $\alpha = \arctan\left(\frac{Y}{X}\right)$ (equation (40)), and by measuring ϕ_c (equation (25)). We take the errors in X and Y to be ± 0.5 holes, and the errors in ϕ_c and ε to be $\pm 1°$. We find that for the first case, $\alpha = 51 \pm 2°$, and thus $n = n_\alpha = 1.53 \pm 0.04$, while measuring the critical angle ϕ_c directly yields $\phi_c = 6 \pm 1°$, meaning that $n = n_{\phi_c} = 1.52 \pm 0.03$.

4.7 Experiment 6

The intensity of the light striking the photosensor is directly proportional to the photosensor's output voltage, with a constant of proportionality that does not change throughout the experiment. For Part A, we find that the unreflected intensity of the laser beam, in terms of the voltage read by the photosensor, is $I_0 = 5.55 \pm 0.05\,V$. We also find that the room lights contribute an offset of $I_{lights} = 20 \pm 5\,mV$.

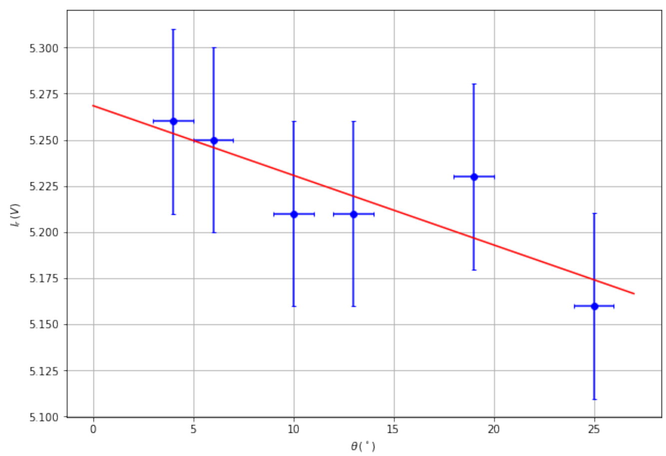

Figure 17: I_r vs θ for the flat mirror. The data points are in blue and the line in red represents the best linear fit.

Figure 17 shows the results of Part C, and the extrapolation to normal incidence gives a value for the reflected intensity $I_r(0)$ of $5.27 \pm 0.02\,V$, and thus the value of the mirror's reflectivity is $R_m = 0.953 \pm 0.004$. The intensity of light at the photosensor for case in which the mirror is placed opposite the beam splitter I_1 was measured to be $336 \pm 5\,mV$, and repeating the same setup using the prism produces an intensity $I_2 = 46 \pm 5\,mV$, so applying equation (45) gives a reflectivity for the prism equal to $R_p = 0.04 \pm 0.01$, which in turn means that the refraction index is $n = 1.49 \pm 0.08$.

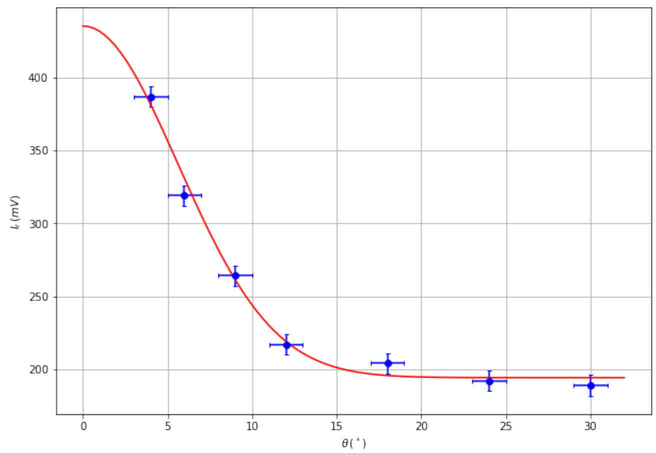

Figure 18: I_r vs θ for the prism. The data points are in blue and the line in red represents the best fit for a model of a Gaussian plus an offset.

Figure 18 shows the results of Part D. Here, we perform the extrapolation to normal incidence in a different way than in the previous part, and instead model the curve as a Gaussian added to an offset. The value of the intensity at $\theta = 0°$, according to this extrapolation, is $I_r(0) = 435 \pm 25\, mV$, which gives a value of $R_p = 0.04 \pm 0.01$, and a value for the refractive index $n = 1.49 \pm 0.02$.

5 Analysis

5.1 Experiment 1

The results of experiment 1 are consistent with the law of reflection, which requires that $\theta_i = \theta_r$, although the agreement is not perfect, as we expected a slope of $m = -2$ and a y-intercept of $b = 90°$ and the results were that $m = -1.92 \pm 0.08$ and $b = 88 \pm 2°$. Even though these expectations are within the error bars, they are at their edge, which suggests that there might be some kind of systematic error involved. Most plausibly, the rotation stage was not zeroed to sufficient precision, and this can introduce a big error, in particular at small angles. It is also possible that the mirror's position with respect to the table was not recorded perfectly, since the mirror is not directly on top of the hole into which its holder is screwed to. More consideration to these sources of error should be applied in the future.

5.2 Experiment 2

Experiment 2's result agrees reasonable well with the expected value for the refractive index of water, $n_w = 1.33$. Sources of error in this experiment include the fact that the water used was not distilled water, and that it was not exactly at $20°\, C$, which are the conditions for which we expect to get $n_w = 1.33$. Another, and potentially more important, source of error is that the container in which the water was held is made of a glass with a non-negligible thickness, and this should certainly contribute to the measured deviation of the laser beam. Finally, the laser beam's ~mm diameter might have introduced errors in the measured position of the spot with respect to the graph paper, as one has to calculate where the center of the spot is by eye. This becomes more complicated as the distance a increases since the spot becomes elongated.

5.3 Experiment 3

The nominal value of the refractive index of the glass prism used in this experiment and the slab used in the next one is $n = 1.517$, so our result for this experiment of $n = 1.51 \pm 0.01$ is totally consistent with expectations, especially given the fact that a single measurement was performed. The minimum deviation was calculated by eye as the point in which increasing or decreasing the angle of the rotation stage led to the refracted laser beam to move away from the prism, and this procedure certainly introduced a degree of error. The X and Y values were measured with a ruler, and the non-zero height of the laser beam also introduced errors as the location of the spot with respect to the table had to be calculated crudely by eye.

5.4 Experiment 4

The results from this experiment are remarkably in line with expectations, as the refractive index is measured to be $n = 1.514 \pm 0.009$, which yields a percent discrepancy of ~0.1%. This is related to the relatively large number of data points used, as well as the extraordinary precision of the micrometer. The principal errors involved are the uncertainties related to reading off the angles from the rotation stage, and getting the voltage measured by the photosensor to come back to its original value, because the voltmeter reading tended to fluctuate and only measured the voltage to a precision of 0.01 V.

5.5 Experiment 5

The two values for n found in this experiment were slightly different, with $n_\alpha = 1.53 \pm 0.04$, and $n_{\phi_c} = 1.52 \pm 0.03$. Both agree well with the expected value for n, although the error bars are larger than in the case of the previous two experiments. This has to do with the relatively large errors involved in the measurements of X, Y, and ϕ_c. In the first case, it would have been preferable to place the beam stopper at a larger distance away from the prism than was done, and in the second case, the fact that the angle is small and the rotation stage's reading is not very precise implies that there is a large error involved in the measurement. The fact that ε is not known to arbitrary precision also contributes to the resulting error.

5.6 Experiment 6

We get values for n of 1.49 ± 0.08 and 1.49 ± 0.02. Both results are consistent with expectations, although the expected value is slightly over the edge of the error bars in the second case. The origin of the large errors in the first case becomes evident upon inspection of Figure 17, which suggests that a more precise voltmeter should have been used, as the variation of the intensity of the reflected beam is very small for the case of the flat mirror. Another possibility would have been dimming the laser beam further, but that would have added a scale factor into the equations because the filter would have had to be removed afterwards given the very small reflectivity of the prism. It is hard to explain why the intensity curve produced by the prism in Figure 18 is so well approximated by a Gaussian. The geometric effect described in section 3.6.3 explains why the intensity does not decrease linearly like in the case of the flat mirror, but it is unclear to us as to why a Gaussian model gives such a good result. It is also noteworthy that both nominal values found for n are the same, and slightly less than the expected value. A more careful repetition of the experiment, with a better control over the sources of error, as well as performing a larger number of measurements, would be useful in order to resolve these issues.

6 Conclusion

We have performed a series of experiments designed to apply some basic laws of optics that have allowed us to measure the refractive index of two different materials and to test the law of reflection. We find the results to be consistent with expectations, and that some experimental methods yield better results than others. In particular, the setup in experiment 4 enabled us to calculate the refractive index of a glass prism to a precision of ~0.1%, which is about 10 times better than the accuracy obtained in the other setups. This reinforces the idea that different ways of measuring the same quantity are not equivalent in terms of their precision, even in the case of experiments performed in closely controlled laboratory conditions.

References

[1] Hecht, E. *Optics*, *5th edit.*, Pearson Education Limited 2017.

[2] Bodenschatz, E., et al. *Modern Experimental Optics Laboratory Manual*, Cornell University Physics Department 2016.

[3] Jones E, Oliphant E, Peterson P, et al. *SciPy: Open Source Scientific Tools for Python,* 2001-, http://www.scipy.org/.

[4] W. H. Press, S. A. Teukolsky, W. T. Vetterling and B. P. Flannery *Numerical Recipes, The Art of Scientific Computing, 3rd edit.*, Camb. Univ. Press 2007.

[5] P. T. Boggs and J. E. Rogers, "Orthogonal Distance Regression," in "Statistical analysis of measurement error models and applications: proceedings of the AMS-IMS-SIAM joint summer research conference held June 10-16, 1989," Contemporary Mathematics, vol. 112, pg. 186, 1990.

[6] Lebigot, E.O. *Uncertainties: a Python package for calculations with uncertainties*, http://pythonhosted.org/uncertainties/